1 # Tail Vein Injections of Recombinant Human Thioredoxin

2 # Prevents High Fat-induced Endothelial Dysfunction in Mice

3 Rob H.P. Hilgers, Assistant Professor, Pharmaceutical Sciences, College of Pharmacy

4 & Health Sciences, Campbell University, Buies Creek, NC

5

6 **Address for correspondence**:

7 Dr. Rob H.P. Hilgers

8 Assistant Professor

9 Pharmaceutical Sciences

10 College of Pharmacy & Health Sciences

11 Post Office Box 1090

12 Ph: (910) 893-1706

13 Fax: (910) 983-1697

14 Email: hilgers@campbell.edu

15

16 **Number of pages: 23**

17 **Number of Figures: 6**

18 **Word count: 6,280**

19

20 **Abstract**

21 **Background** – Obesity is a serious risk factor for cardiovascular diseases. A high fat diet

22 results in cellular oxidative stress and endothelial dysfunction in resistance-sized arteries,

23 characterized by reduced nitric oxide (NO) and endothelium-dependent hyperpolarizing

24 (EDH) responses. Thioredoxin-1, a sulfo-oxidoreductase protein that cleaves disulfide

25 bridges between two adjacent cysteine residues in oxidized proteins, has been shown to

26 lower blood pressure and improve endothelium-dependent relaxing responses in aged

27 C57Bl6/J mice.

28 **Methods and Results** − Young (~ 3 month-old) male C57Bl6/J mice were fed a high fat

29 diet (42% kcal from fat; obese) or a normal chow (lean) for 3 months. Mice were

30 administered recombinant human thioredoxin-1 (rhTrx; 25 mg/kg) or saline (0.9% NaCl)

31 via tail vein injection at the start, after one month, and after two months. Body weight

32 (BW) was comparable between lean/rhTrx1 and lean/saline at the time of euthanasia (32

33 ±1 g versus 32 ± 1 g). The high fat regimen resulted in a comparable BW between

34 obese/saline and obese/rhTrx mice (47 ± 1 g versus 45 ± 2 g, respectively). Small

35 (second-order branches) mesenteric arteries (MA2), coronary and femoral arteries were

36 isolated and mounted on the wire-myograph. MA2 and femoral arteries from obese/saline

37 had blunted acetylcholine (10^{-9} – 10^{-5} M)-mediated relaxations compared to lean/saline

38 mice, but not to the NO donor sodium nitroprusside. NO and EDH-mediated relaxing

39 responses were blunted in MA2 from obese/lean mice compared to the three other

40 groups.

41 **Conclusion** – Tail vein injections with rhTrx prevented endothelial dysfunction in obese

42 mice by improving NO and EDH relaxing responses in MA2.

43   In resistance-sized arteries (< 250 μm in lumen diameter) relaxation is mediated via

44   endothelium-derived factors such as NO and prostacyclin (PGI_2), but also by a conductive

45   electro-coupled pathway, called endothelium-dependent hyperpolarization (EDH), that is

46   associated with a propagation of endothelial and smooth muscle cell hyperpolarization

47   [1]. Endothelial calcium-activated potassium channels (K_{Ca}) initiate and propagate this

48   EDH response [1]. In the endothelium of small mesenteric arteries, small-conductance

49   K_{Ca} (SK_{Ca}) and intermediate-conductance K_{Ca} (IK_{Ca}) are solely responsible for this EDH

50   [2]. In isometric wire-myography this EDH can be assessed in a contracted artery

51   segment followed by endothelial K_{Ca} opening under conditions where NO and PGI_2

52   release is inhibited. Under pathological conditions, including obesity, the contribution of

53   these endothelium-derived mediators is compromised (for a review see [3, 4]). An altered

54   cellular reduction-oxidation (redox) balance shifted towards a more oxidative state is

55   presumed to be the culprit of this endothelial dysfunction [5, 6]. Thiol/disulfide redox

56   changes of specific amino acids, most notably cysteine, modulate the activity of many

57   enzymes [7]. Thioredoxin-1 (Trx) is a 12-kDa cytosolic oxidoreductase capable of

58   reducing disulfide bridges between two adjacent cysteine residues, hereby keeping

59   cysteine groups in its active thiol (reduced) formation [8]. Overexpression of human Trx

60   in mice has been elegantly shown to reduce age-related hypertension [9], to increase

61   endothelium-dependent acetylcholine-mediated relaxations in the mesenteric vascular

62   bed [9, 10] and to preserve endothelial nitric oxide synthase (eNOS) activity via a

63   reductive deglutathionylation process [11]. In addition, the EDH response was enhanced

64   in small mesenteric arteries derived from these Trx transgenic mice compared to their

65   wild-type littermates [10]. These observations suggest that Trx maintains the activity of

66   eNOS and endothelial K_{Ca} channels. In this study it was hypothesized that tail vein

67   injections of recombinant human Trx (rhTrx) would protect against a high fat diet-induced

68   impairment in endothelium-dependent relaxation in resistance-sized arteries in C57Bl6/J

69   mice. In this study, attention was focused on the role of endothelium-derived NO and EDH

70   relaxing responses in mediating ACh- and NS309-induced relaxations in murine arteries

71   derived from lean and obese mice with or without intervention with rhTrx.

Methods

Animals and tail vein injections

Male C57Bl6/J mice (10 – 12 weeks) were placed on either a normal chow (lean group) or a high fat diet (obese group). The high fat (42% kcal from fat) diet was purchased from Harlan Laboratories (Teklad Custom Research Diet TD.88137). Mice were divided in four groups: lean/saline, obese/saline, lean/rhTrx, and obese/rhTrx. In the saline groups, mice were injected via the tail vein with saline (100 μL of a 0.9% NaCl sterile solution), and for the rhTrx group with recombinant human Thioredoxin-1 (R&D Systems; 2.5 mg/kg in 100 μL solution in 0.9% NaCl solution). Mice were briefly placed in a holding chamber and anesthetized with isoflurane (1.5% delivered in 100% O_2). The tail was heated with a light source in order to dilate the tail vein. Tail vein injections were performed with insulin syringes (Exel, 30G). After one and two months the tail vein injections were repeated. After three months mice were euthanized. All procedures were approved by the IACUC at Campbell University and were consistent with the *Guide for the Care and Use of Laboratory Animals* published by the National Institute of Health. All animals were maintained on a standard 12-h light/12-h dark cycle, in a temperature-controlled barrier facility.

Isolation of arteries and isometric wire-myography

Mice were euthanized via CO_2 inhalation and the mesentery and heart were dissected. From the left upper leg a 2 mm segment of the femoral artery was dissected. The mesentery was placed in a Petri dish fill with black silicon and ice-cold Krebs Ringer Buffer (KRB) with the following composition (in mM): 118.5 NaCl, 4.7 KCl, 2.5 $CaCl_2$, 1.2 $MgSO_4$,

94   1.2 KH_2PO_4, 25.0 $NaHCO_3$, and 5.5 D-glucose. Second-order branches of the superior

95   mesenteric artery (MA2) were dissected. From the heart a 1.5 − 2 mm-segment of the left

96   descending coronary artery was dissected. Segments were mounted on a wire-myograph

97   (Danish Myotechnology Inc, Model 620M, Aarhus, Denmark) and stretched to their

98   optimal internal circumference as described earlier [9]. Force (mN) generated by stretch

99   was corrected for vessel length to obtain tension values in mN/mm. Vessel length was

100   measured in the myograph chamber with the help of a scale bar in the ocular of the stereo

101   dissecting microscope. After an incubation period of 60 minutes, arteries were "woken

102   up" by replacing KRB with 60 mM KCl in KRB (replacing equimolar NaCl with KCl), thus

103   generating a stable tension after a few minutes. This tension level (minus the baseline

104   tension) was set as 100% contraction (as % of K_{60}). Cumulative concentration-response

105   curves (CRC) were performed with phenylephrine (PHE; 0.01 – 30 μM) for MA2, and

106   serotonin (5-HT; 0.001 – 3 μM) for coronary and femoral arteries. Cumulative CRC to

107   acetylcholine (ACh; 0.001 – 10 μM) were assessed in contracted artery segments in the

108   absence of any inhibitors. Endothelium-independent relaxations were assessed with CRC

109   to the NO donor sodium nitroprusside (0.1 nM – 10 μM) in the presence of the non-

110   selective NO synthase blocker N^{ω}-nitro-L-arginine methyl ester (L-NAME; 100 μM) and

111   the non-selective cyclo-oxygenase inhibitor indomethacin (10 μM).

112   **Protocol to isolate the contribution of NO in PHE-induced contractions and ACh-**

113   **induced relaxing responses in MA2**

114   The contribution of NO in PHE-induced contractions and ACh-induced relaxations was

115   assessed by comparing the area between the curves (ABC) of the individual

116   concentration-response curves (CRCs) in the absence and presence of the L-NAME. To

117 rule out any contribution of vasoactive prostaglandins, all segments were treated with

118 indomethacin in the reminder of this study.

Protocol to isolate the contribution of EDH in ACh- and NS309-induced relaxing

120 **responses in MA2**

121 The EDH response was blocked with selective inhibitors of small-conductance and

122 intermediate-conductance calcium-activated potassium channels (SK_{Ca} and IK_{Ca},

123 respectively) by UCL-1684 (1 μM) and TRAM-34 (10 μM), respectively. Both inhibitors

124 were incubated for 30 minutes prior CRC to ACh. The EDH-mediated relaxing responses

125 were assessed by calculating ABC between the individual CRCs to ACh and the direct

126 endothelial K_{Ca} opener NS309 [12] in the absence and presence of TRAM-34 and UCL-

127 1684. Another protocol was designed to assess EDH responses in MA2 that were

128 incubated with L-NAME. The remaining relaxing responses to ACh and NS309 is an

129 indication for the contribution of the EDH response in the absence of NO and vasoactive

130 prostaglandins.

Data and statistical analysis

132 Data are shown as mean ± SEM. Concentration-response curves were analyzed with

133 two-way analysis of variance (ANOVA) followed by Bonferroni post-hoc test or Tukey's

134 test for multiple comparisons. Other values were analyzed by paired and unpaired

135 Student's t test. $P < 0.05$ was considered to be statistically significant. Sensitivity (pEC_{50})

136 to ACh and NS309 was determined in GraphPad Prism (version 7) using nonlinear

137 regression (variable slope with four parameters; constrains: TOP: 100, BOTTOM, 0).

138

139 **Results**

140 **Comparable body weight after 3 months of a high fat diet regimen**

141 The average age at euthanization was similar for all four mice groups (28 ± 1 g for

142 lean/saline, 28 ± 1 g for obese/saline, 28 ± 1 g for lean/rhTrx, and 28 ± 2 g for

143 obese/rhTrx). Body weight progressively increased during the 3-month high fat regimen

144 or normal diet in both saline-infused and rhTrx-injected mice (Figure 1A). The body weight

145 gain was roughly 15 g for mice placed on a high fat diet for 13 weeks (Figure 1B). Tail

146 vein injection of rhTrx did not result in a statistically significantly different body weight gain

147 compared to saline injection (Figure 1B).

148

149 **Tail vein injection of rhTrx prevents high fat-induced inward remodeling of small**

150 **mesenteric arteries**

151 Second-order branches of the superior mesenteric artery (MA2) from all 4 experimental

152 groups were mounted on an isometric wire-myograph system. Following incubation for

153 30 min, arteries were stretched as described in the Methods section. Optimal diameters

154 from MA2 from obese/saline mice were statistically significantly reduced compared to

155 their lean counterparts (Figure 1C; 168 ± 5 μm versus 184 ± 5 μm, respectively). Infusion

156 of rhTrx prevented this inward remodeling after a high-fat diet, since optimal diameters

157 were comparable for both lean and obese mice that were given rhTrx (Figure 1C; 183 ±

158 5 μm versus 182 ± 4 μm, respectively). Active wall tension (in mN/mm) in response to a

159 depolarizing KRB solution containing 60 mM KCl were comparable in MA2 for all

160 experimental mice groups (Figure 1D). Coronary artery optimal diameter (Figure 1E) and

161   active wall tension (Figure 1F) were similar for the four experimental mice groups,

162   although wall tensions tended to be larger in the obese/rhTrx group (Figure 1F). Femoral

163   artery optimal diameter tended to be smaller in the obese/saline group compared to the

164   other three groups (Figure 1G), but active wall tension were statistically significantly

165   reduced compared to the other three groups (Figure 1H).

166

Contractile responses are comparable for all experimental groups

168   Phenylephrine contracted MA2 in a concentration-dependent manner (Figure 2A).

169   Normalized (as percentage of 60 mM KCl) concentration-response curves (CRC) showed

170   no significant differences in both sensitivity (pEC_{50}) and maximum contraction (E_{max}) for

171   PHE in all groups (Figure 1). Serotonin (5-HT) contracted coronary and femoral arteries

172   in a concentration-dependent manner (Figure 2). Similarly to MA2, no significant

173   differences in pEC_{50} and E_{max} were observed between the experimental groups for both

174   artery types.

175

Acetylcholine-induced relaxing responses are impaired in MA2 and femoral arteries from obese/saline mice, but not in obese/rhTrx mice

178   Acetylcholine relaxed MA2, coronary and femoral arteries in a concentration-dependent

179   manner (Figure 3A – 3C). This relaxation was diminished in MA2 and femoral arteries,

180   but not coronary arteries, derived from obese mice injected with saline. In MA2, pEC_{50}

181   was decreased 10-fold in obese/saline compared to lean/saline (5.45 ± 0.08 versus 6.55

182   ± 0.05; $P < 0.05$; Figure 3A). E_{max} was significantly diminished in obese/saline compared

183 to lean/saline ($58 \pm 6\%$ versus $85 \pm 3\%$; $P < 0.05$; Figure 3A). ACh-induced relaxations

184 were comparable in MA2 between lean/saline and lean/rhTrx mice (Figure 3A). Strikingly,

185 tail vein infusion of rhTrx completely prevented the high fat-induced ACh-induced

186 impairment, with pEC_{50} and E_{max} values similar to lean/saline values (6.25 ± 0.08 and 75

187 $\pm 7\%$, respectively; Figure 3A). A similar trend was observed in femoral arteries, but the

188 differences were not as pronounced as in MA2 (Figure 3C). ACh-induced relaxations in

189 coronary arteries were comparable for all experimental groups (Figure 3B). The observed

190 impairments in ACh-induced relaxations were endothelium-dependent since relaxing

191 responses to sodium nitroprusside, a NO donor with endothelium-independent relaxing

192 properties, were not statistically significant between all groups for MA2, coronary and

193 femoral arteries (Figure 3D – 3F).

194

NO release is diminished in MA2 from obese/saline mice, but preserved in

196 **obese/rhTrx**

197 The suppressing role of endothelial derived NO in PHE-induced contractions was

198 analyzed by comparing CRCs to PHE in the absence and presence of L-NAME. Figure

199 4A to 4D shows contractions to PHE for MA2 derived from the four groups. The area

200 between the curves is highlighted in light blue. In a similar fashion, the role of NO in ACh-

201 mediated relaxing responses was assessed. Figure 4E to 4H shows ACh-induced

202 relaxing responses in the absence and presence of L-NAME with the light blue areas as

203 area between the curves. The area under/above the curves (AUC for PHE or AAC for

204 ACh) and the arbitrary units of the areas between the curves are depicted in Figure 4I to

205 4L. The surface area of the light blue areas are smaller for MA2 from obese/saline mice

206   (Figure 4G, 4E, and 4J) compared to the other three groups, highlighting a diminished

207   functional role of NO in vasomotor responses. More importantly, the role of NO in these

208   responses is completely protected by tail vein injections of rhTrx (Figure 4D, 4H, and 4L).

209

210   **EDH relaxing responses are diminished in obese/saline, but preserved in**

211   **obese/rhTrx**

212   The contribution of endothelial K_{Ca} channels on the EDH relaxing response was

213   determined via two pharmacological approaches. The first approach assesses

214   differences between CRCs to ACh and NS309 in the absence and presence of the two

215   endothelial K_{Ca} channel blockers TRAM-34 and UCL-1684. Figure 5A to 5D shows the

216   contribution of endothelial K_{Ca} channels that were activated indirectly via ACh-induced

217   signaling for the four groups. The yellow highlighted areas show the ABC and are an

218   indication of the magnitude of endothelial K_{Ca} involvement in response to ACh. The middle

219   panel of graphs (Figure 5E to 5H) depict the contribution of these K_{Ca} channels after direct

220   opening by NS309, with the magnitude of the EDH response highlighted in yellow. The

221   areas under the curve (AUC) for all graphs are summarized in the bar graphs (Figure 5I

222   to 5L). The extent of the yellow highlighted areas are shown as differences between bar

223   heights. No significant difference between the bar graphs was observed for obese/saline

224   mice, indicating blunted EDH response in these vessels (Figure 5J). Tail vein injections

225   of rhTrx completely prevented the high fat-induced reduction in the EDH response (Figure

226   5L).

227 Historically, the EDH-mediated response is analyzed in the presence of L-NAME and

228 indomethacin. Figure 6A shows that ACh-induced EDH responses were smallest in MA2

229 from obese/saline mice. AAC values were significantly reduced in MA2 from obese/saline

230 compared to the other groups (Figure 6B). Sensitivity for ACh was significantly lower in

231 MA2 from obese/saline mice compared to the other groups (Figure 6C). NS309-induced

232 relaxing responses were reduced in MA2 from obese/saline mice compared to the other

233 groups (Figure 6D). AAC (Figure 6E) and sensitivity (Figure 6F) for NS309 were

234 significantly decreased in obese/saline compared to the other groups. Again, tail vein

235 injections of rhTrx completely prevented the high fat-induced blunted EDH response.

236

Discussion

237

238 The present isometric myograph functional data support the hypothesis that tail vein

239 injections of human recombinant thioredoxin completely protects against high fat-induced

240 endothelial dysfunction in small mesenteric and femoral arteries. In small mesenteric

241 arteries this protection is characterized by an increased NO and EDH relaxing response,

242 the latter via enhanced endothelial K_{Ca} channel opening.

243 Obesity is a major risk factor for the development of cardiovascular and metabolic

244 complications such as hypertension and type 2 diabetes [13, 14]. This mouse strain is

245 well suited because of its high sensitivity for obesity and type 2 diabetes in response to a

246 high fat diet [15]. The objective of this study was not to assess plasma triglycerides and

247 cholesterol levels, weigh subcutaneous and epididymal fat mass in order to confirm a

248 metabolic syndrome. Here an obesity-induced diet (42% kcal from fat) was used to elicit

249 an endothelial dysfunction in small arteries derived from C57Bl6/J mice. This was

250 successful since small mesenteric and skeletal femoral arteries isolated from saline-

251 injected obese mice presented classical signs of endothelial dysfunction: blunted ACh-

252 induced relaxing responses. Judged from the comparable body weight gain during the 13

253 week high fat diet for saline- or rhTrx-injected obese mice, the injection of rhTrx did not

254 have a significant impact on body mass gain. A dose of 25 mg/kg of rhTrx was chosen to

255 inject via the tail vein. This dose was comparable to the dose used before, which resulted

256 in detectable plasma levels and a blood pressure lowering effect in aged hypertensive

257 mice [9].

258 Resistance arteries play a crucial role in blood pressure regulation and local tissue

259 perfusion, as well as their capacity to adapt to hemodynamic changes (*e.g.* pressure,

260 stretch and flow) [16, 17]. The optimal diameters of second-order mesenteric arteries

261 (MA2) derived from obese/saline mice were significantly smaller than their lean

262 counterparts, suggesting inward remodeling during obesity. Inward remodeling of small

263 arteries has been observed in patients with essential hypertension [18], in cerebral

264 arteries of obese rats [19], and in mesenteric arteries that underwent surgical blood flow

265 cessation [20]. The optimal diameters were determined via horizontal stretching of

266 isolated arteries in the wire-myograph. No pressure-myography and morphological

267 analysis were performed to prove that the observed smaller optimal diameters were in

268 fact the result of anatomical structural adaptations to obesity. Coronary and femoral

269 arteries had similar optimal diameters for the four experimental groups, which suggests

270 a regio heterogeneous effect.

271 Contractile responses in the absence of any inhibitors were unaltered irrespective

272 of diet and treatment in MA2, coronary and femoral arteries. However, endothelium-

273 dependent ACh-induced relaxing responses were impaired in MA2 and femoral arteries

274 derived from obese/saline compared to the three counterparts. Endothelium-independent

275 relaxing responses by the NO donor sodium nitroprusside were comparable for all groups

276 and artery types. These observations demonstrate that the observed differences in ACh-

277 induced responses were manifested at the level of the endothelium.

278 The mesenteric arterial bed is prone to high fat-induced impairment in

279 endothelium-dependent relaxation, probably due to the close proximity of intestinal

280 absorption of fatty acids. The small mesenteric artery is a preferred choice of resistance-

281 sized artery for the vascular biologist due to its abundance and relative ease of dissection.

282 Hence, endothelial dysfunction in response to obesity has been shown in murine small

283 mesenteric arteries [21-25], but some studies did not observe an impairment in ACh-

284 induced relaxation [26-28]. Similarly, a high-fat diet has been shown to result in either

285 preserved endothelial function [29, 30] or impaired endothelial function in murine coronary

286 arteries [31, 32]. Similar to this study, impaired ACh-induced relaxing responses in

287 femoral arteries were observed in C57Bl6/J mice that received a high fat diet [30].

288 A pharmacological approach was used to assess the role of NO and the

289 endothelium-dependent hyperpolarizing (EDH) relaxing response in MA2. In general,

290 indomethacin is used in ex $vivo$ vascular reactivity studies to block cyclo-oxygenases that

291 produce vasoactive prostaglandins. Here, all MA2 were treated with indomethacin to rule

292 out any contribution of vasoactive prostaglandins. In the present study, the main

293 mechanism of endothelium-dependent relaxation in the murine small mesenteric artery

294 was via NO release and EDH, which is in agreement with other studies [10, 33, 34]. In

295 obese and saline-injected mice, both the NO- and EDH-dependent relaxation in MA2

296 were significantly impaired compared to lean and saline-injected mice. This observation

297 is congruent with other studies using a high fat diet and small mesenteric arteries in the

298 myograph [21, 22, 35]. EDH responses were assessed with both ACh (indirectly) and

299 NS309 (directly), a non-selective endothelial IK_{Ca} and SK_{Ca} channel opener [12]. ACh

300 increases intracellular Ca^{2+} ions in endothelial cells that activate endothelial K_{Ca} channels,

301 whereas NS309 is an opener of these K_{Ca} channels. In murine small mesenteric arteries,

302 the IK_{Ca} (or IK1) channel contributes mainly to ACh-stimulated Ca^{2+} dynamics [36] and

303 genetic knockdown of IK1 reduces ACh-induced EDH response in murine mesenteric

304 arteries [37, 38]. In agreement with these observations, the NS309-induced EDH

305 response was inhibited by TRAM-34 and not by UCL-1684 (data not shown), confirming

306   the importance of the IK_{Ca} channel in this species and artery type. The IK_{Ca} channel can

307   be oxidized by hydrogen peroxide (H_2O_2) and other chemical cysteine thiol oxidizers, like

308   5,5'-dithio-bis (2-nitrobenzoic acid) (DTNB or Ellman's reagent) or [(O-

309   carboxyphenyl)thio]ethyl mercury sodium salt (thimerosal), to inhibit IK_{Ca} channel activity

310   in bovine aortic endothelial cells [39]. Thiol reducing agents like dithiotreitol or reduced

311   glutathione were able to restore the IK_{Ca} channel activity. *In vivo*, the IK_{Ca} channel can be

312   inactivated by oxidative stress factors like obesity and hyperhomocysteinemia [40, 41].

313   Interestingly, the nonluminal S6 region of the IK_{Ca} channel protein, which is crucial in

314   pore-forming, contains two adjacent cysteine residues (Cys276 and -277), which have

315   the potential to become subject to post-translational thiol modification [42]. The above

316   observations suggest redox modulation of the IK_{Ca} channel with an important modulatory

317   role for thioredoxin. Using transgenic mice overexpressing human thioredoxin-1 (Trx-Tg),

318   an enhanced EDH response was observed in MA2 compared to non-transgenic mice [10].

319   Furthermore, endothelial NO release was enhanced in aortae of Trx-Tg mice [9]. These

320   observations prompted the idea of exogenously administrating rhTrx in mice in an effort

321   to study whether rhTrx could protect against high fat-induced endothelial dysfunction.

322   Tail vein injection of rhTrx completely protected endothelium-dependent relaxing

323   responses in MA2 against a high fat diet, via an increased NO release and enhanced

324   EDH response. The latter was mediated via endothelial K_{Ca} channel activation. This

325   observation strongly suggests that redox modulation of cysteine thiol groups on proteins

326   regulates the release of endothelial-derived NO and EDH. Trx is also an antioxidant,

327   because it scavenges hydroxyl radicals [43]. It could therefore be argued that the

328   beneficial effects observed by rhTrx are attributed to its antioxidant activity. However,

329   dominant-negative Trx mice, which express a mutant Trx without the catalytic two

330   cysteine residues, but still possess radical scavenging properties, display blunted EDH-

331   mediated relaxing responses in MA2 [10]. Whether Trx directly modulates K_{Ca} channel

332   activity needs to be elucidated. A novel IK_{Ca} selective positive-gating modulator, SKA-31

333   [44], potentiated the EDH response in porcine coronary arteries, suggesting the important

334   role of the IK_{Ca} channel in this artery [45]. Hence, Trx may have beneficial protective

335   effects on coronary blood flow during conditions that reduce expression of endothelial K_{Ca}

336   channels, such as diabetes [46-48] and hypertension [49-51].

337   In conclusion, tail vein injection of rhTrx completely protected obese mice from

338   high fat-induced endothelial dysfunction. In addition, compared to lean/saline-injected

339   mice, NO and EDH-mediated responses were enhanced in MA2 from obese/rhTrx-

340   injected mice. These vasoprotective actions of Trx may provide a promising therapeutic

341   potential in the combat of oxidative stress-linked pathologies.

342

Acknowledgement

346

347

348   **Figure Legends**

349   **Figure 1**. Body weight (in g) increases during the 3-month diet regimens (**A**) and body

350   weight at the time of euthanization (**B**) for the four experimental groups. Optimal

351   diameters (in μm) for MA2 (**C**), coronary (**E**), and femoral arteries (**G**) obtained via

352   isometric myography. Active wall tension (in mN/mm) in response to 60 mM KCl in KRB

353   for MA2 (**D**), coronary (**F**), and femoral arteries (**H**). Values are expressed in mean $\pm$

354   S.E.M. * P < 0.05 obese/saline versus lean/saline; # P < 0.05 obese/saline versus

355   obese/rhTrx.

356   **Figure 2**. Contractile responses to the α_1-adrenergic agonist phenylephrine (PHE; 0.01

357   – 30 μM) in MA2 (**A**), coronary (**B**) and femoral arteries (**C**) for the four experimental

358   groups. Values are expressed in mean $\pm$ S.E.M.

359   **Figure 3**. Endothelium-dependent ACh-induced relaxation in MA2 (**A**), coronary (**B**) and

360   femoral arteries (**C**) for the four experimental groups. Endothelium-independent

361   relaxations to the NO donor sodium nitroprusside (SNP) in MA2 (**D**), coronary (**E**) and

362   femoral arteries (**F**) for the four experimental groups. Values are expressed in mean $\pm$

363   S.E.M. * P < 0.05 obese/saline versus the three other groups.

364   **Figure 4**. Contribution of NO in vasomotor responses. Contractile responses to the α_1-

365   adrenergic agonist phenylephrine (PHE; 0.01 – 30 μM) in MA2 in the absence (CON,

366   open circles) and presence of L-NAME (100 μM, closes circles) for lean/saline (**A**),

367   obese/saline (**B**), lean/rhTrx (**C**) and obese/rhTrx mice (**D**). Endothelium-dependent ACh-

368   induced relaxation in MA2 in the absence (CON) and presence L-NAME (100 μM) for

369   lean/saline (**E**), obese/saline (**F**), lean/rhTrx (**G**) and obese/rhTrx mice (**H**). Hghlighted

370   blue areas represent the contribution of NO. Calculated area under the curve (AUC) for

371   PHE-induced contractions (black) and calculated area above the curve (AAC) for ACh-

372   induced (purple) responses for lean/saline (**I**), obese/saline (**J**), lean/rhTrx (**K**) and

373   obese/rhTrx mice (**L**). Differences in AAC or AUC (Δ) are shown. All arteries were

374   incubated with indomethacin (10 μM). Values are expressed in mean ± S.E.M. * $P < 0.05$,

375   # $P < 0.001$, NS is not significant.

376   **Figure 5**. Contribution of EDH. Endothelium-dependent ACh-induced (**A** to **D**) and

377   NS309-induced (**E** to **H**) relaxing responses in MA2 in the absence (CON, open symbols)

378   and the presence of TRAM-34 (10 μM) + UCL-1684 (1 μM) (closed circles) for lean/saline

379   (**A** and **E**), obese/saline (**B** and **F**), lean/rhTrx (**C** and **G**), and obese/rhTrx (**D** and **H**). Light

380   blue areas represents the contribution of EDH via endothelial K_{Ca} channel activation.

381   Calculated area under the curve (AUC) for ACh-induced responses (black) and NS309-

382   induced responses (green) for lean/saline (**I**), obese/saline (**J**), lean/rhTrx (**K**) and

383   obese/rhTrx mice (**L**). Differences in AUC (Δ) are shown. All arteries were incubated with

384   indomethacin (10 μM). Values are expressed in mean ± S.E.M. * $P < 0.05$, # $P < 0.001$,

385   NS is not significant.

386   **Figure 6**. Endothelium-dependent ACh-induced (**A** to **C**) and NS309-induced (**D** to **F**)

387   relaxing responses in MA2 in the presence of L-NAME in lean/saline (open black circles

388   or bars), obese/saline (closed black circles or bars), lean/rhTrx (open blue circles or bars),

389   and obese/rhTrx (closed blue circles or bars). Area above the curve are summarized in

390   (**B** and **E**). Sensitivity (pEC_{50}) are summarized in (**C** and **F**). All arteries were incubated

391   with indomethacin (10 μM). Values are expressed in mean ± S.E.M. * $P < 0.05$

392   obese/saline versus all other groups.

References

1.   Garland CJ, Dora KA. EDH: endothelium-dependent hyperpolarization and microvascular signalling. Acta Physiol (Oxf). 2017;219(1):152-61. Epub 2016/01/12. doi: 10.1111/apha.12649. PubMed PMID: 26752699.

2.   Crane GJ, Gallagher N, Dora KA, Garland CJ. Small- and intermediate-conductance calcium-activated K+ channels provide different facets of endothelium-dependent hyperpolarization in rat mesenteric artery. J Physiol. 2003;553(Pt 1):183-9. Epub 2003/10/14. doi: 10.1113/jphysiol.2003.051896. PubMed PMID: 14555724; PubMed Central PMCID: PMCPMC2343487.

3.   Coleman HA, Tare M, Parkington HC. Endothelial potassium channels, endothelium-dependent hyperpolarization and the regulation of vascular tone in health and disease. Clin Exp Pharmacol Physiol. 2004;31(9):641-9. Epub 2004/10/14. doi: 10.1111/j.1440-1681.2004.04053.x. PubMed PMID: 15479173.

4.   Goto K, Ohtsubo T, Kitazono T. Endothelium-Dependent Hyperpolarization (EDH) in Hypertension: The Role of Endothelial Ion Channels. Int J Mol Sci. 2018;19(1). Epub 2018/01/25. doi: 10.3390/ijms19010315. PubMed PMID: 29361737; PubMed Central PMCID: PMCPMC5796258.

5.   Kanaan GN, Harper ME. Cellular redox dysfunction in the development of cardiovascular diseases. Biochim Biophys Acta Gen Subj. 2017;1861(11 Pt A):2822-9. Epub 2017/08/06. doi: 10.1016/j.bbagen.2017.07.027. PubMed PMID: 28778485.

6.   Munzel T, Camici GG, Maack C, Bonetti NR, Fuster V, Kovacic JC. Impact of Oxidative Stress on the Heart and Vasculature: Part 2 of a 3-Part Series. J Am Coll Cardiol. 2017;70(2):212-29. Epub 2017/07/08. doi: 10.1016/j.jacc.2017.05.035. PubMed PMID: 28683969; PubMed Central PMCID: PMCPMC5663297.

7.   Hanschmann EM, Godoy JR, Berndt C, Hudemann C, Lillig CH. Thioredoxins, glutaredoxins, and peroxiredoxins--molecular mechanisms and health significance: from cofactors to antioxidants to redox signaling. Antioxid Redox Signal. 2013;19(13):1539-605. Epub 2013/02/13. doi: 10.1089/ars.2012.4599. PubMed PMID: 23397885; PubMed Central PMCID: PMCPMC3797455.

8.   Holmgren A. Thioredoxin. Annu Rev Biochem. 1985;54:237-71. Epub 1985/01/01. doi: 10.1146/annurev.bi.54.070185.001321. PubMed PMID: 3896121.

9.   Hilgers RH, Kundumani-Sridharan V, Subramani J, Chen LC, Cuello LG, Rusch NJ, et al. Thioredoxin reverses age-related hypertension by chronically improving vascular redox and restoring eNOS function. Sci Transl Med. 2017;9(376). Epub 2017/02/10. doi: 10.1126/scitranslmed.aaf6094. PubMed PMID: 28179506; PubMed Central PMCID: PMCPMC5808940.

10.   Hilgers RH, Das KC. Role of in vivo vascular redox in resistance arteries. Hypertension. 2015;65(1):130-9. Epub 2014/10/15. doi: 10.1161/HYPERTENSIONAHA.114.04473. PubMed PMID: 25312439; PubMed Central PMCID: PMCPMC4268237.

11.   Subramani J, Kundumani-Sridharan V, Hilgers RH, Owens C, Das KC. Thioredoxin Uses a GSH-independent Route to Deglutathionylate Endothelial Nitric-oxide Synthase and Protect against Myocardial Infarction. J Biol Chem. 2016;291(45):23374-89. Epub 2016/09/03. doi: 10.1074/jbc.M116.745034. PubMed PMID: 27587398; PubMed Central PMCID: PMCPMC5095395.

12.   Strobaek D, Teuber L, Jorgensen TD, Ahring PK, Kjaer K, Hansen RS, et al. Activation of human IK and SK Ca2+ -activated K+ channels by NS309 (6,7-dichloro-1H-indole-2,3-dione 3-oxime). Biochim Biophys Acta. 2004;1665(1-2):1-5. Epub 2004/10/09. doi: 10.1016/j.bbamem.2004.07.006. PubMed PMID: 15471565.

13.   Li M, Qian M, Xu J. Vascular Endothelial Regulation of Obesity-Associated Insulin Resistance. Front Cardiovasc Med. 2017;4:51. Epub 2017/08/30. doi: 10.3389/fcvm.2017.00051. PubMed PMID: 28848738; PubMed Central PMCID: PMCPMC5552760.
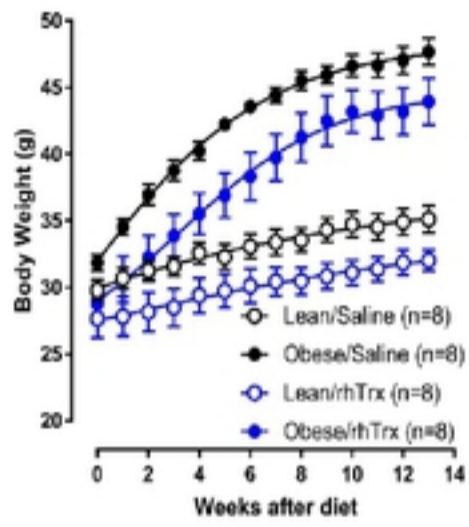
437   14.   Alpert MA, Omran J, Bostick BP. Effects of Obesity on Cardiovascular Hemodynamics, Cardiac
438   Morphology, and Ventricular Function. Curr Obes Rep. 2016;5(4):424-34. Epub 2016/10/17. doi:
439   10.1007/s13679-016-0235-6. PubMed PMID: 27744513.
440   15.   Collins S, Martin TL, Surwit RS, Robidoux J. Genetic vulnerability to diet-induced obesity in the
441   C57BL/6J mouse: physiological and molecular characteristics. Physiol Behav. 2004;81(2):243-8. Epub
442   2004/05/26. doi: 10.1016/j.physbeh.2004.02.006. PubMed PMID: 15159170.
443   16.   Henrion D. Pressure and flow-dependent tone in resistance arteries. Role of myogenic tone. Arch
444   Mal Coeur Vaiss. 2005;98(9):913-21. Epub 2005/10/20. PubMed PMID: 16231579.
445   17.   De Mey JG, Schiffers PM, Hilgers RH, Sanders MM. Toward functional genomics of flow-induced
446   outward remodeling of resistance arteries. Am J Physiol Heart Circ Physiol. 2005;288(3):H1022-7. Epub
447   2005/02/12. doi: 10.1152/ajpheart.00800.2004. PubMed PMID: 15706039.
448   18.   Schofield I, Malik R, Izzard A, Austin C, Heagerty A. Vascular structural and functional changes in
449   type 2 diabetes mellitus: evidence for the roles of abnormal myogenic responsiveness and dyslipidemia.
450   Circulation. 2002;106(24):3037-43. Epub 2002/12/11. PubMed PMID: 12473548.
451   19.   Deutsch C, Portik-Dobos V, Smith AD, Ergul A, Dorrance AM. Diet-induced obesity causes cerebral
452   vessel remodeling and increases the damage caused by ischemic stroke. Microvasc Res. 2009;78(1):100-
453   6. Epub 2009/04/21. doi: 10.1016/j.mvr.2009.04.004. PubMed PMID: 19374911; PubMed Central PMCID:
454   PMCPMC3959658.
455   20.   Pourageaud F, De Mey JG. Structural properties of rat mesenteric small arteries after 4-wk
456   exposure to elevated or reduced blood flow. Am J Physiol. 1997;273(4 Pt 2):H1699-706. Epub 1997/11/15.
457   PubMed PMID: 9362233.
458   21.   Aoqui C, Chmielewski S, Scherer E, Eissler R, Sollinger D, Heid I, et al. Microvascular dysfunction in
459   the course of metabolic syndrome induced by high-fat diet. Cardiovasc Diabetol. 2014;13:31. Epub
460   2014/02/05. doi: 10.1186/1475-2840-13-31. PubMed PMID: 24490784; PubMed Central PMCID:
461   PMCPMC3916304.
462   22.   Tian XY, Wong WT, Xu A, Lu Y, Zhang Y, Wang L, et al. Uncoupling protein-2 protects endothelial
463   function in diet-induced obese mice. Circ Res. 2012;110(9):1211-6. Epub 2012/03/31. doi:
464   10.1161/CIRCRESAHA.111.262170. PubMed PMID: 22461387.
465   23.   Dunn SM, Hilgers RH, Das KC. Decreased EDHF-mediated relaxation is a major mechanism in
466   endothelial dysfunction in resistance arteries in aged mice on prolonged high-fat sucrose diet. Physiol Rep.
467   2017;5(23). Epub 2017/12/08. doi: 10.14814/phy2.13502. PubMed PMID: 29212858; PubMed Central
468   PMCID: PMCPMC5727270.
469   24.   Wang H, Luo W, Wang J, Guo C, Wang X, Wolffe SL, et al. Obesity-induced endothelial dysfunction
470   is prevented by deficiency of P-selectin glycoprotein ligand-1. Diabetes. 2012;61(12):3219-27. Epub
471   2012/08/15. doi: 10.2337/db12-0162. PubMed PMID: 22891216; PubMed Central PMCID:
472   PMCPMC3501858.
473   25.   Gil-Ortega M, Condezo-Hoyos L, Garcia-Prieto CF, Arribas SM, Gonzalez MC, Aranguez I, et al.
474   Imbalance between pro and anti-oxidant mechanisms in perivascular adipose tissue aggravates long-term
475   high-fat diet-derived endothelial dysfunction. PLoS One. 2014;9(4):e95312. Epub 2014/04/25. doi:
476   10.1371/journal.pone.0095312. PubMed PMID: 24760053; PubMed Central PMCID: PMCPMC3997398.
477   26.   Eichhorn B, Muller G, Leuner A, Sawamura T, Ravens U, Morawietz H. Impaired vascular function
478   in small resistance arteries of LOX-1 overexpressing mice on high-fat diet. Cardiovasc Res. 2009;82(3):493-
479   502. Epub 2009/03/18. doi: 10.1093/cvr/cvp089. PubMed PMID: 19289377.
480   27.   Ellis A, Cheng ZJ, Li Y, Jiang YF, Yang J, Pannirselvam M, et al. Effects of a Western diet versus high
481   glucose on endothelium-dependent relaxation in murine micro- and macro-vasculature. Eur J Pharmacol.
482   2008;601(1-3):111-7. Epub 2008/11/11. doi: 10.1016/j.ejphar.2008.10.042. PubMed PMID: 18996368.
483   28.   Soares AG, de Carvalho MHC, Akamine E. Obesity Induces Artery-Specific Alterations: Evaluation
484   of Vascular Function and Inflammatory and Smooth Muscle Phenotypic Markers. Biomed Res Int.

485   2017;2017:5038602. Epub 2017/05/04. doi: 10.1155/2017/5038602. PubMed PMID: 28466012; PubMed
486   Central PMCID: PMCPMC5390568.

487   29.   Feher A, Rutkai I, Beleznai T, Ungvari Z, Csiszar A, Edes I, et al. Caveolin-1 limits the contribution
488   of BK(Ca) channel to EDHF-mediated arteriolar dilation: implications in diet-induced obesity. Cardiovasc
489   Res. 2010;87(4):732-9. Epub 2010/03/20. doi: 10.1093/cvr/cvq088. PubMed PMID: 20299334; PubMed
490   Central PMCID: PMCPMC2920808.

491   30.   Bender SB, Castorena-Gonzalez JA, Garro M, Reyes-Aldasoro CC, Sowers JR, DeMarco VG, et al.
492   Regional variation in arterial stiffening and dysfunction in Western diet-induced obesity. Am J Physiol
493   Heart Circ Physiol. 2015;309(4):H574-82. Epub 2015/06/21. doi: 10.1152/ajpheart.00155.2015. PubMed
494   PMID: 26092984; PubMed Central PMCID: PMCPMC4537938.

495   31.   Dou H, Feher A, Davila AC, Romero MJ, Patel VS, Kamath VM, et al. Role of Adipose Tissue
496   Endothelial ADAM17 in Age-Related Coronary Microvascular Dysfunction. Arterioscler Thromb Vasc Biol.
497   2017;37(6):1180-93. Epub 2017/05/06. doi: 10.1161/ATVBAHA.117.309430. PubMed PMID: 28473444;
498   PubMed Central PMCID: PMCPMC5484536.

499   32.   Gamez-Mendez AM, Vargas-Robles H, Rios A, Escalante B. Oxidative Stress-Dependent Coronary
500   Endothelial Dysfunction in Obese Mice. PLoS One. 2015;10(9):e0138609. Epub 2015/09/19. doi:
501   10.1371/journal.pone.0138609. PubMed PMID: 26381906; PubMed Central PMCID: PMCPMC4575160.

502   33.   Dora KA, Sandow SL, Gallagher NT, Takano H, Rummery NM, Hill CE, et al. Myoendothelial gap
503   junctions may provide the pathway for EDHF in mouse mesenteric artery. J Vasc Res. 2003;40(5):480-90.
504   Epub 2003/10/30. doi: 10.1159/000074549. PubMed PMID: 14583659.

505   34.   Godo S, Sawada A, Saito H, Ikeda S, Enkhjargal B, Suzuki K, et al. Disruption of Physiological Balance
506   Between Nitric Oxide and Endothelium-Dependent Hyperpolarization Impairs Cardiovascular
507   Homeostasis in Mice. Arterioscler Thromb Vasc Biol. 2016;36(1):97-107. Epub 2015/11/07. doi:
508   10.1161/ATVBAHA.115.306499. PubMed PMID: 26543099.

509   35.   Brondum E, Kold-Petersen H, Simonsen U, Aalkjaer C. NS309 restores EDHF-type relaxation in
510   mesenteric small arteries from type 2 diabetic ZDF rats. Br J Pharmacol. 2010;159(1):154-65. Epub
511   2009/12/18. doi: 10.1111/j.1476-5381.2009.00525.x. PubMed PMID: 20015296; PubMed Central PMCID:
512   PMCPMC2823361.

513   36.   Qian X, Francis M, Kohler R, Solodushko V, Lin M, Taylor MS. Positive feedback regulation of
514   agonist-stimulated endothelial Ca2+ dynamics by KCa3.1 channels in mouse mesenteric arteries.
515   Arterioscler Thromb Vasc Biol. 2014;34(1):127-35. Epub 2013/11/02. doi: 10.1161/ATVBAHA.113.302506.
516   PubMed PMID: 24177326; PubMed Central PMCID: PMCPMC4181598.

517   37.   Brahler S, Kaistha A, Schmidt VJ, Wolfle SE, Busch C, Kaistha BP, et al. Genetic deficit of SK3 and
518   IK1 channels disrupts the endothelium-derived hyperpolarizing factor vasodilator pathway and causes
519   hypertension. Circulation. 2009;119(17):2323-32. Epub 2009/04/22. doi:
520   10.1161/CIRCULATIONAHA.108.846634. PubMed PMID: 19380617.

521   38.   Si H, Heyken WT, Wolfle SE, Tysiac M, Schubert R, Grgic I, et al. Impaired endothelium-derived
522   hyperpolarizing factor-mediated dilations and increased blood pressure in mice deficient of the
523   intermediate-conductance Ca2+-activated K+ channel. Circ Res. 2006;99(5):537-44. Epub 2006/07/29.
524   doi: 10.1161/01.RES.0000238377.08219.0c. PubMed PMID: 16873714.

525   39.   Cai S, Sauve R. Effects of thiol-modifying agents on a K(Ca2+) channel of intermediate conductance
526   in bovine aortic endothelial cells. J Membr Biol. 1997;158(2):147-58. Epub 1997/07/15. PubMed PMID:
527   9230092.

528   40.   Zhao L, Wang Y, Ma X, Wang Y, Deng X. Oxidative stress impairs IKCa- and SKCa-mediated
529   vasodilatation in mesenteric arteries from diabetic rats. Nan Fang Yi Ke Da Xue Xue Bao. 2013;33(7):939-
530   44. Epub 2013/07/31. PubMed PMID: 23895829.

531   41.   Cheng Z, Jiang X, Kruger WD, Pratico D, Gupta S, Mallilankaraman K, et al. Hyperhomocysteinemia
532   impairs endothelium-derived hyperpolarizing factor-mediated vasorelaxation in transgenic cystathionine
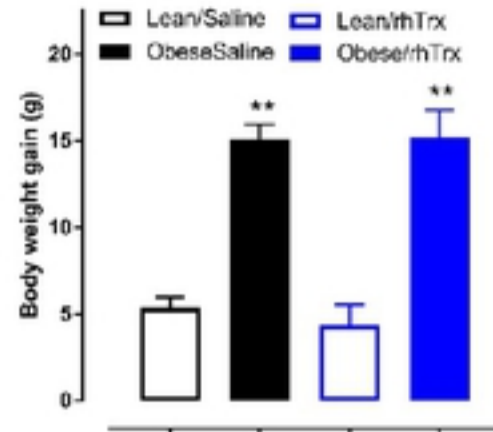
533   beta synthase-deficient mice. Blood. 2011;118(7):1998-2006. Epub 2011/06/10. doi: 10.1182/blood-
534   2011-01-333310. PubMed PMID: 21653942; PubMed Central PMCID: PMCPMC3158725.

535   42.   Klein H, Garneau L, Banderali U, Simoes M, Parent L, Sauve R. Structural determinants of the
536   closed KCa3.1 channel pore in relation to channel gating: results from a substituted cysteine accessibility
537   analysis. J Gen Physiol. 2007;129(4):299-315. Epub 2007/03/14. doi: 10.1085/jgp.200609726. PubMed
538   PMID: 17353352; PubMed Central PMCID: PMCPMC2151617.

539   43.   Das KC, Das CK. Thioredoxin, a singlet oxygen quencher and hydroxyl radical scavenger: redox
540   independent functions. Biochem Biophys Res Commun. 2000;277(2):443-7. Epub 2000/10/18. doi:
541   10.1006/bbrc.2000.3689. PubMed PMID: 11032742.

542   44.   Sankaranarayanan A, Raman G, Busch C, Schultz T, Zimin PI, Hoyer J, et al. Naphtho[1,2-d]thiazol-
543   2-ylamine (SKA-31), a new activator of KCa2 and KCa3.1 potassium channels, potentiates the
544   endothelium-derived hyperpolarizing factor response and lowers blood pressure. Mol Pharmacol.
545   2009;75(2):281-95. Epub 2008/10/29. doi: 10.1124/mol.108.051425. PubMed PMID: 18955585; PubMed
546   Central PMCID: PMCPMC2635097.

547   45.   Olivan-Viguera A, Valero MS, Pinilla E, Amor S, Garcia-Villalon AL, Coleman N, et al. Vascular
548   Reactivity Profile of Novel KCa 3.1-Selective Positive-Gating Modulators in the Coronary Vascular Bed.
549   Basic Clin Pharmacol Toxicol. 2016;119(2):184-92. Epub 2016/01/29. doi: 10.1111/bcpt.12560. PubMed
550   PMID: 26821335; PubMed Central PMCID: PMCPMC5720859.

551   46.   Burnham MP, Johnson IT, Weston AH. Impaired small-conductance Ca2+-activated K+ channel-
552   dependent EDHF responses in Type II diabetic ZDF rats. Br J Pharmacol. 2006;148(4):434-41. Epub
553   2006/05/10. doi: 10.1038/sj.bjp.0706748. PubMed PMID: 16682967; PubMed Central PMCID:
554   PMCPMC1751791.

555   47.   Liu Y, Cole V, Lawandy I, Ehsan A, Sellke FW, Feng J. Decreased coronary arteriolar response to
556   KCa channel opener after cardioplegic arrest in diabetic patients. Mol Cell Biochem. 2018;445(1-2):187-
557   94. Epub 2018/01/07. doi: 10.1007/s11010-017-3264-x. PubMed PMID: 29305679; PubMed Central
558   PMCID: PMCPMC6033646.

559   48.   Weston AH, Absi M, Harno E, Geraghty AR, Ward DT, Ruat M, et al. The expression and function
560   of Ca(2+)-sensing receptors in rat mesenteric artery; comparative studies using a model of type II diabetes.
561   Br J Pharmacol. 2008;154(3):652-62. Epub 2008/04/17. doi: 10.1038/bjp.2008.108. PubMed PMID:
562   18414396; PubMed Central PMCID: PMCPMC2439515.

563   49.   Gschwend S, Henning RH, de Zeeuw D, Buikema H. Coronary myogenic constriction antagonizes
564   EDHF-mediated dilation: role of KCa channels. Hypertension. 2003;41(4):912-8. Epub 2003/03/19. doi:
565   10.1161/01.HYP.0000063883.83470.7B. PubMed PMID: 12642510.

566   50.   Fujii K, Tominaga M, Ohmori S, Kobayashi K, Koga T, Takata Y, et al. Decreased endothelium-
567   dependent hyperpolarization to acetylcholine in smooth muscle of the mesenteric artery of
568   spontaneously hypertensive rats. Circ Res. 1992;70(4):660-9. Epub 1992/04/01. PubMed PMID: 1551193.

569   51.   Hilgers RH, Webb RC. Reduced expression of SKCa and IKCa channel proteins in rat small
570   mesenteric arteries during angiotensin II-induced hypertension. Am J Physiol Heart Circ Physiol.
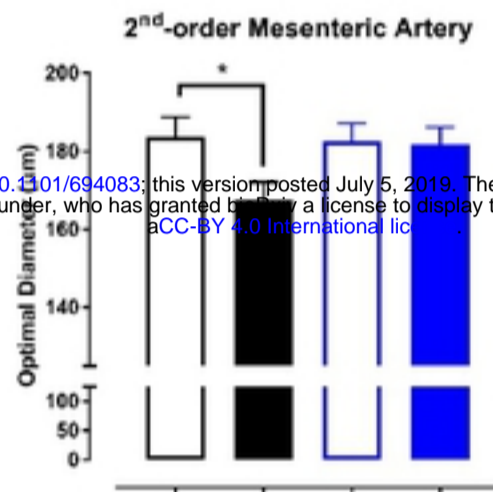571   2007;292(5):H2275-84. Epub 2007/01/09. doi: 10.1152/ajpheart.00949.2006. PubMed PMID: 17209000.
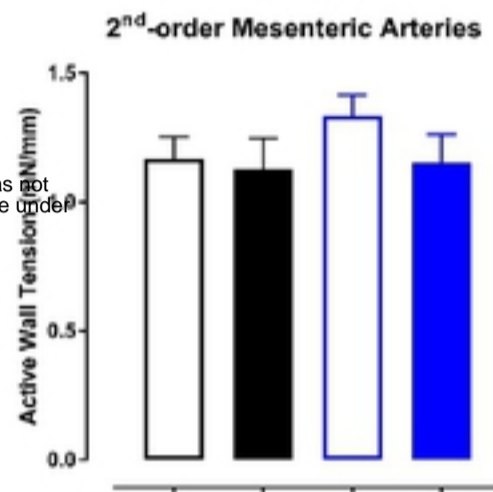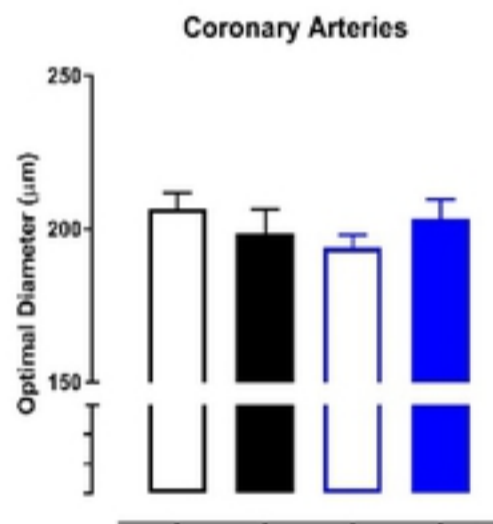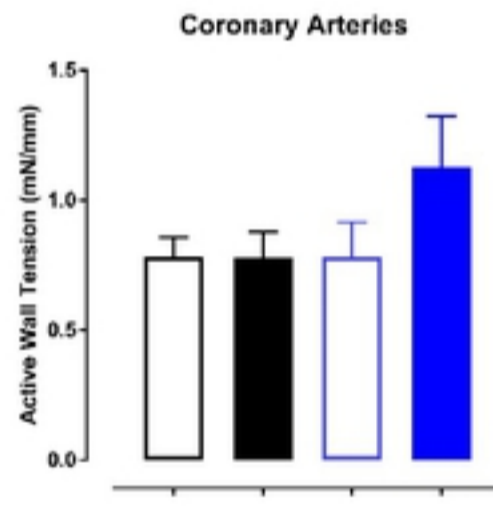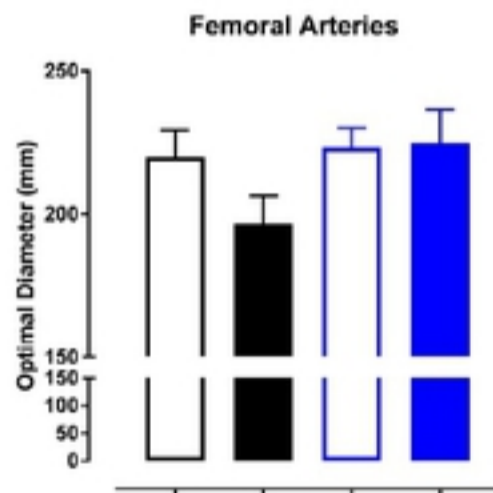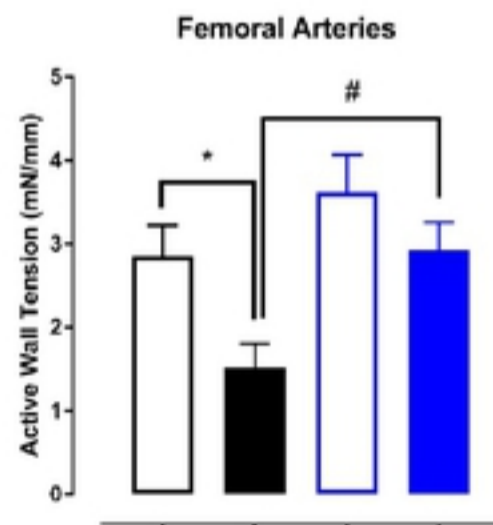
572

Figure 1

Figure 1

Figure 2

A 2nd-order Mesenteric Arteries
- Lean/Saline
- Obese/Saline
- Lean/rhTrx
- Obese/rhTrx

B Coronary Arteries
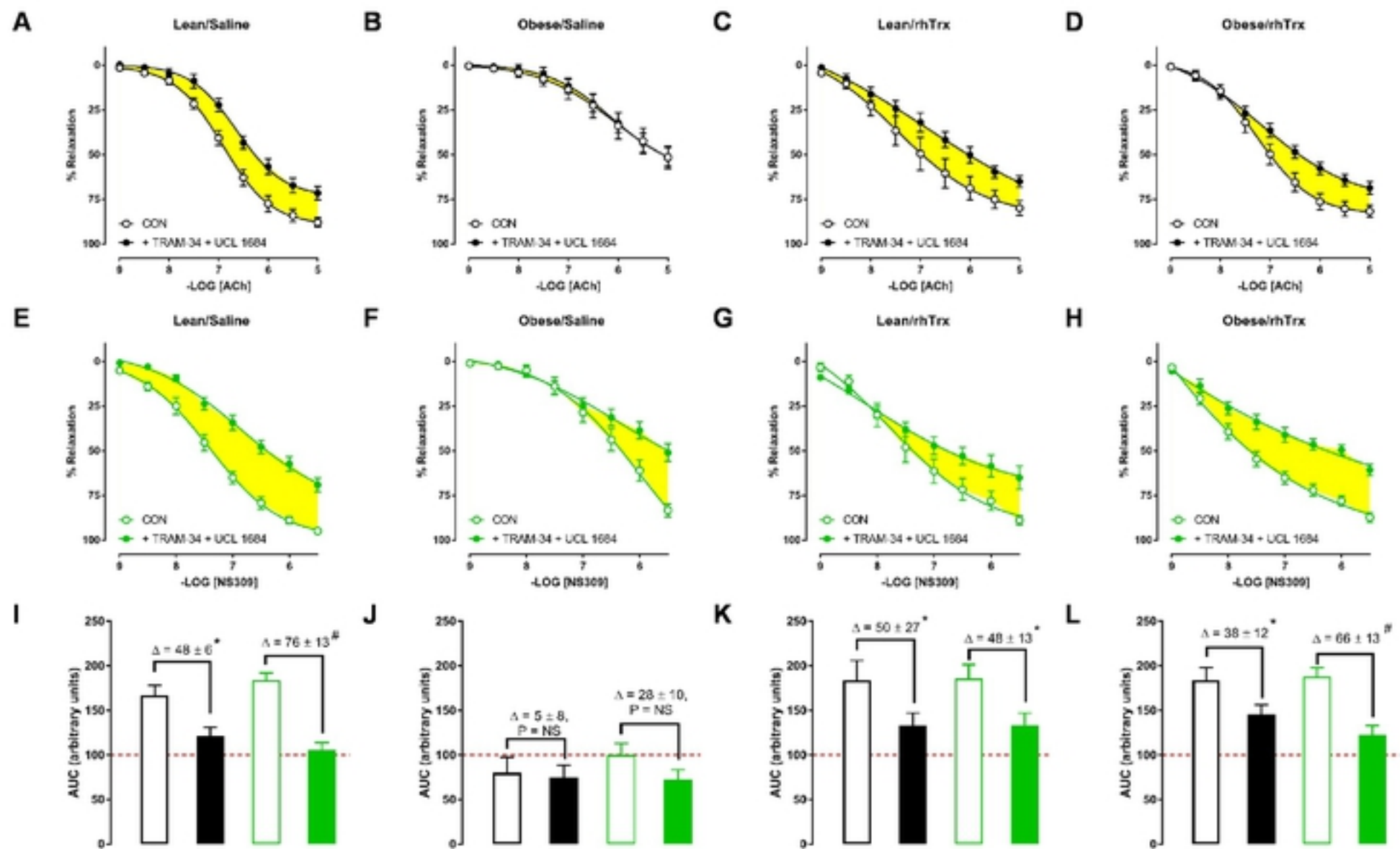
C Femoral Arteries
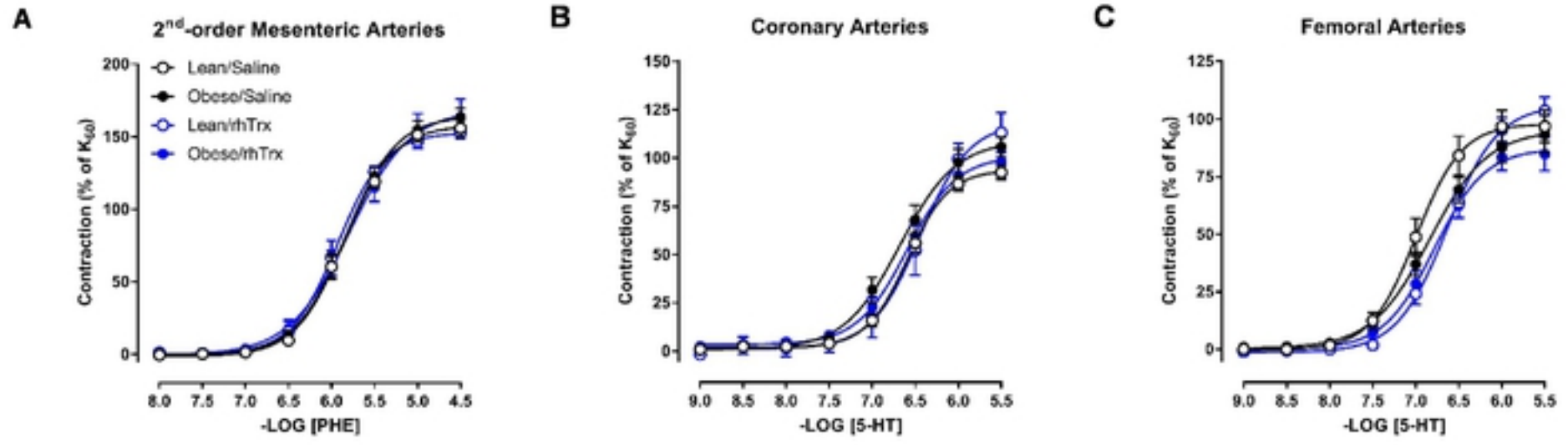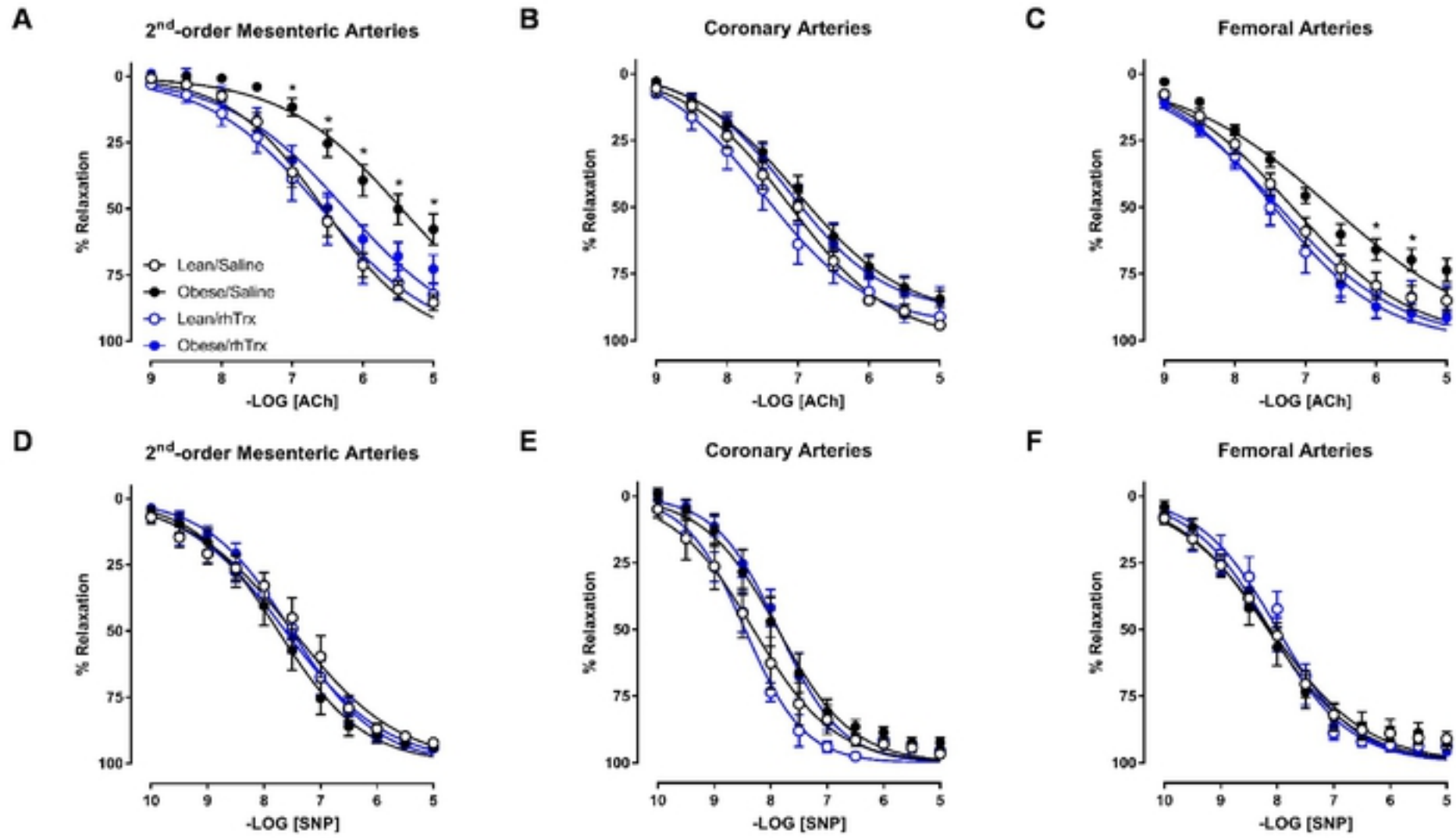
Figure 2

Figure 3

Figure 3
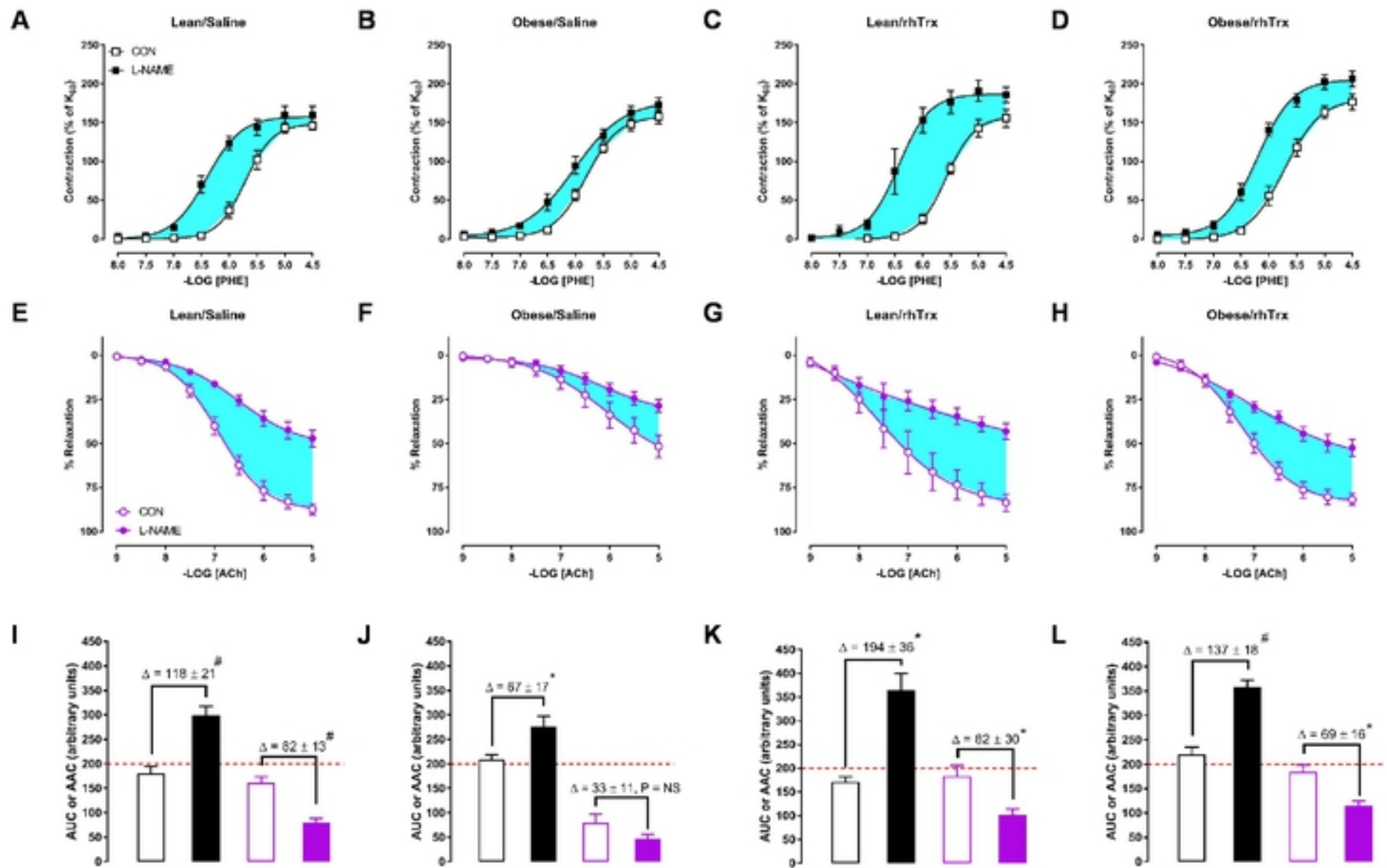
Figure 4

Figure 5

Figure 5

Figure 6

Figure 6